Quantum Electronics **39** (10) 917 – 922 (2009)

NONLINEAR OPTICAL PHENOMENA

PACS numbers: 42.50.Gy; 42.50.Md
DOI: 10.1070/QE2009v039n10ABEH014025

Adiabatons in the nonstationary double resonance on degenerate quantum transitions

A.V. Volkov, N.A. Druzhinina, O.M. Parshkov

***Abstract*. The nonstationary double resonance is numerically simulated in the Λ-scheme of degenerate energy levels with the quantum number *J* of the total angular momentum equal to 0, 2, and 1. The analysis is performed in the slowly varying envelope approximation taking into account the inhomogeneous broadening of quantum transition lines. In the case of a high-power input low-frequency pulse of long duration with a flat top switched on before the application of a comparatively weak and short input high-frequency pulse and switched off after the end of the latter, a specific pulsed structure, the so-called double adiabaton, can appear. It differs from an adiabaton known from the theory of electromagnetically induced transparency by the decomposition of the high-frequency pulse into two pulses with oppositely directed elliptic polarisations.**

Keywords: *degeneracy of energy levels, elliptic polarisation of radiation, inhomogeneous broadening, adiabaton.*

1. Introduction

A double resonance in laser fields is the resonance interaction of two laser radiations with two quantum transitions sharing an energy level. The study of a nonstationary double resonance in the fields of short pulses has revealed a number of pulsed structures such as simultons [1, 2], Raman solitons [3], and pulses with complete energy transfer from one pulse to another [4]. Extensive investigations of the phenomenon of electromagnetically induced transparency (EIT), which is a particular case of the double resonance, included the description of pulsed structures such as consistent pulses [5], adiabatons [6], super-slow pulses [7], and dark polaritons [8]. The use of such pulsed structures opens up new possibilities for the development of a quantum memory [9 – 11] and controlling laser radiation parameters [12 – 14].

Theoretical studies of the nonstationary double resonance were based, as a rule, on the model of quantum transitions involving nondegenerate energy levels. Such an approach excludes effects related to a change in the polarisation state of pulses during their propagation. The nonstationary double resonance on degenerate quantum transitions was studied in papers [15, 16]. By using the method of inverse scattering problem, the authors of these papers found solutions of the simulton type for the system of equations describing this process.

The aim of our paper is to simulate numerically effects appearing in the nonstationary double resonance on degenerate energy levels taking into account a possible change in the polarisation states of interacting radiations. Unlike studies [15, 16], we take into account the inhomogeneous broadening of quantum transition lines and the inequality of their oscillator strengths at which the system of evolution equations cannot be integrated by the method of inverse scattering problem [15]. It is assumed that energy levels are characterised in the order of their increasing energy by the quantum numbers $J = 0$, 2, 1 of the total angular momentum operator, the upper level being shared by two resonantly excited quantum transitions (the Λ interaction scheme). Irreversible relaxation processes are neglected. It is assumed that a high-power low-frequency input radiation pulse of long duration with a flat top is switched on before the application of a comparatively weak and short high-frequency input pulse and is switched off after the end of the latter. Simulations are performed for the Λ-scheme of energy levels of the ^{202}Pb isotope, in which EIT was observed for circularly polarised laser fields [17]. This Λ-scheme was chosen for the theoretical analysis due to its simplicity and the possibility of experimental verification of the obtained results. This study is a continuation of investigations [18] in which the input low-frequency radiation was weaker than the input high-frequency radiation.

2. Formulation of the boundary-value problem

The three-level Λ-scheme, consisting of the nondegenerate ($J = 0$) lower, five-fold degenerate ($J = 2$) middle, and triply degenerate ($J = 1$) upper levels, is formed, for example, by the 6p^2 ^{3}P$_0$, 6p^2 ^{3}P$_2$, and 6p7s ^{3}P$^{\circ}_1$ levels of the ^{208}Pb isotope. Let M be the quantum number of the operator of the projection of the total angular momentum on the z axis, and ϕ_k ($k = 1, 2, ..., 9$) be the orthonormalised set of the common eigenfunctions of the Hamiltonian and operators of the total angular momentum and its projection on the z axis for an isolated atom, which correspond to the lower ($k = 1$, $M = 0$), upper ($k = 2, 3, 4$, $M = -1, 0, 1$, respectively) and middle ($k = 5, 6, ..., 9$, $M = -2, -1, 0, 1, 2$, respectively) levels. Let D_1 and D_2 be the reduced electric dipole moments for the $J = 0 \rightarrow J = 1$ and $J = 2 \rightarrow J = 1$ transitions, respec-

A.V. Volkov, N.A. Druzhinina, O.M. Parshkov Saratov State Technical University, ul. Politekhnicheskaya 77, 410054 Saratov, Russia; e-mail: oparshkov@mail.ru

Received 17 December 2008; revision received 17 March 2009
Kvantovaya Elektronika **39** (10) 917 – 922 (2009)
Translated by M.N. Sapozhnikov

tively, and ω_1 and ω_2 be the frequencies of these transitions for an atom at rest ($\omega_1 > \omega_2$). By assuming that the resonance medium is a rarefied gas, we introduce the notation $T_1 = 2/\Delta_1$, where Δ_1 is the width (at the e^{-1} height level) of the Doppler density distribution of transition frequencies ω_1'.

We represent the electric field of two laser pulses propagating along the z axis with carrier frequencies ω_1 and ω_2 in the form

$$\boldsymbol{E} = \sum_{l=1}^{2} \mu_l [\boldsymbol{i} E_{xl} \cos(\omega_l t - k_l z + \delta_{xl}) + \boldsymbol{j} E_{yl} \cos(\omega_l t - k_l z + \delta_{yl})], \tag{1}$$

where $\mu_l = \mathrm{h}\sqrt{2l+1}/(|D_l|T_1)$; $\boldsymbol{i}$ and $\boldsymbol{j}$ are the unit vectors of the x and y axes; E_{xl}, E_{yl}, δ_{xl}, δ_{yl} are functions of z and t; and $k_l = \omega_1/c$. Because $\omega_1 > \omega_2$, radiation at frequency ω_1 is the high-frequency radiation, while radiation at frequency ω_2 is the low-frequency radiation.

The wave function of an atom can be written in the form

$$\Psi = \bar{c}_1 \phi_1 + \left(\sum_{k=2}^{4} \bar{c}_k \phi_k \right) \exp(-\mathrm{i}\xi_1) + \left(\sum_{k=5}^{9} \bar{c}_k \phi_k \right) \exp[-\mathrm{i}(\xi_1 - \xi_2)], \tag{2}$$

where $\xi_l = \omega_l t - k_l z$. Let us introduce variables f_l and g_l and quantities c_i:

$$f_l = [E_{xl} \exp(\mathrm{i}\delta_{xl}) - \mathrm{i}E_{yl} \exp(\mathrm{i}\delta_{yl})]/\sqrt{2},$$

$$g_l = [E_{xl} \exp(-\mathrm{i}\delta_{xl}) - \mathrm{i}E_{yl} \exp(-\mathrm{i}\delta_{yl})]/\sqrt{2},$$

$$c_1 = -2\bar{c}_1 \arg D_1,\; c_2 = \bar{c}_2,\; c_4 = \bar{c}_4,\; c_5 = 2\bar{c}_5 \arg D_2,$$

$$c_7 = (2/\sqrt{6})\bar{c}_7 \arg D_2,\; c_9 = 2\bar{c}_9 \arg D_2.$$

Let us define the normalised independent variables s and w as

$$s = z/z_0,\; w = (t - z/c)/T_1, \tag{3}$$

where $z_0 = 3\mathrm{h}c/(2\pi N|D_1|^2 T_1 \omega_1)$ and N is the concentration of atoms. By describing the evolution of the field and atoms with the help of Maxwell and Schrödinger equations, respectively, we obtain, in the slowly varying amplitude approximation, the system of equations

$$\frac{\partial f_1}{\partial s} = \frac{\mathrm{i}}{\sqrt{\pi}} \int_{-\infty}^{+\infty} c_1 c_2^* \exp(-\varepsilon_1^2) \mathrm{d}\varepsilon_1,$$

$$\frac{\partial f_2}{\partial s} = -\frac{\mathrm{i}}{\sqrt{\pi}} \xi \int_{-\infty}^{+\infty} (c_4^* c_9 + c_2^* c_7) \exp(-\varepsilon_1^2) \mathrm{d}\varepsilon_1,$$

$$\frac{\partial g_1}{\partial s} = \frac{\mathrm{i}}{\sqrt{\pi}} \int_{-\infty}^{+\infty} c_1^* c_4 \exp(-\varepsilon_1^2) \mathrm{d}\varepsilon_1,$$

$$\frac{\partial g_2}{\partial s} = -\frac{\mathrm{i}}{\sqrt{\pi}} \xi \int_{-\infty}^{+\infty} (c_2 c_5^* + c_4 c_7^*) \exp(-\varepsilon_1^2) \mathrm{d}\varepsilon_1,$$

$$\frac{\partial c_1}{\partial w} = -\mathrm{i}(f_1 c_2 - g_1^* c_4),$$

$$\frac{\partial c_2}{\partial w} + \mathrm{i}\varepsilon_1 c_2 = -\frac{\mathrm{i}}{4}(f_1^* c_1 + g_2 c_5 - f_2^* c_7), \tag{4}$$

$$\frac{\partial c_4}{\partial w} + \mathrm{i}\varepsilon_1 c_4 = \frac{\mathrm{i}}{4}(g_1 c_1 - g_2 c_7 + f_2^* c_9),$$

$$\frac{\partial c_5}{\partial w} + \mathrm{i}\varepsilon_1 (1-\beta) c_5 = -\mathrm{i} g_2^* c_2,$$

$$\frac{\partial c_7}{\partial w} + \mathrm{i}\varepsilon_1 (1-\beta) c_7 = \frac{\mathrm{i}}{6}(f_2 c_2 - g_2^* c_4),$$

$$\frac{\partial c_9}{\partial w} + \mathrm{i}\varepsilon_1 (1-\beta) c_9 = \mathrm{i} f_2 c_4.$$

Here,

$$\varepsilon_1 = T_1(\omega_1' - \omega_1);\; \beta = \frac{\omega_2}{\omega_1};\; \xi = \frac{3}{5} \frac{\omega_2 |D_2|^2}{\omega_1 |D_1|^2}.$$

The amplitudes $\bar{c}_3$, $\bar{c}_6$, and $\bar{c}_8$ do not enter into system (4). Their evolution is determined by the closed system of three differential equations, which for the initial conditions $\bar{c}_3 = \bar{c}_6 = \bar{c}_8 = 0$, has the trivial solution $\bar{c}_3 = \bar{c}_6 = \bar{c}_8 = 0$ for all s and w. Integrals in the right-hand sides of the first four equations of system (4) are introduced to take into account the Doppler broadening by averaging the dipole moments of individual atoms over the parameter ε_1, which is uniquely related to the thermal velocity of each atom directed along the z axis. For the chosen transitions of the ^{208}Pb isotope, according to [19], $\beta = 0.7$ and $\xi = 2.11$.

The use of the plane wave approximation in our paper is justified by the fact that in most experiments on the nonstationary double resonance the laser beams of comparatively low intensity with rather large cross sections are employed. For example, it is in this approximation that all the main results of the EIT theory were obtained [20]. The slowly varying amplitude approximation assumes the use of long enough laser pulses so that the values of E_{xl}, E_{yl}, δ_{xl}, δ_{yl}, and $\bar{c}_k$ weakly change during the light oscillation cycle and over the light wavelength [21, 22]. We took all these factors into account in our dimensional estimates in Section 4.

Let us analyse the solutions of system (4) in terms of parameters a_l, α_l, and γ_l of the polarisation ellipses (PEs) of high-frequency ($l = 1$) and low-frequency ($l = 2$) radiations. Here, a_l is the major semiaxis of the PE measured in the units of μ_l; α_l is its inclination angle to the x axis; γ_l is the compression parameter; and $a_l \geqslant 0$, $0 \leqslant \alpha_l < \pi$, $-1 \leqslant \gamma_l \leqslant 1$ [23]. The parameter $|\gamma_l|$ in the ratio of the minor PE axis to its major axis, and the condition $0 < \gamma_l < 1$ ($-1 < \gamma_l < 0$) corresponds to the right-hand (left-hand) elliptic polarisation, while $\gamma_l = 0$ corresponds to linearly polarised radiation. By specifying a_l, α_l, γ_l and one of the phases, for example δ_{xl}, we can uniquely determine the values of f_l and g_l. The parameters of the PE are generally the functions of s and w, which vary slowly over the temporal and spatial periods of the carrier quasi-harmonic.

For $|\gamma_l| = 1$ (circular polarisation), the angle α_l is not defined. The unavoidable small errors in the calculation of γ_l for $|\gamma_l| \approx 1$ lead to considerable errors in the determination of α_l. To avoid these errors, we ascribed to α_l the value outside the interval $0 \leqslant \alpha_l < \pi$, namely, assuming that $\alpha_l = -0.1$ when $|\gamma_l| > 0.99$, i.e. when the PE transforms virtually to a circle. Therefore, the appearance of the negative value of α_l in the dependences means the uncertainty of the angle α_l at the instant when radiation is circularly polarised. If polarisation was elliptic before this moment, the angle α_l changes jump-wise from a value lying in the interval $0 \leqslant \alpha_l < \pi$ to $\alpha_l = -0.1$. The jump-wise change of α_l from $\alpha_l = -0.1$ to $0 \leqslant \alpha_l < \pi$ occurs when circular polarisation transforms to circular polarisation. If the rotating major axis of the PE coincides with the x axis and continues its rotation in the same direction, the angle α_l experiences a jump by $\pm\pi$. The sign of the jump depends on the rotation direction.

The initial conditions ($w = 0$) for system (4) are specified in the form

$$c_1/2 = 1,\ c_2 = c_4 = c_5 = c_7 = c_9 = 0,\ s \geqslant 0,$$

which corresponds to the state in which all the atoms occupy the lower energy level at the initial instant of time. The boundary conditions ($s = 0$) are

$$\alpha_l = \alpha_{l0},\ \gamma_l = \gamma_{l0},\ \delta_{xl} = 0,\ a_l = a_{l0}(w),\ w \geqslant 0, \tag{5}$$

where $l = 1, 2$ and α_{l0} and γ_{l0} are constants. Equalities (5) correspond to input laser pulses with a fixed orientation of the major axis and constant eccentricity of the PE, whereas functions $a_{l0}(w)$ determine the time evolution of the major semiaxis of this ellipse for high-frequency ($l = 1$) and low-frequency ($l = 2$) pulses at the input to the resonance medium.

As additional radiation parameters, we use below the fluence I_l of high-frequency ($l = 1$) and low-frequency ($l = 2$) pulses measured in the units of $c\mu_1^2/(8\pi)$ and their energy W_l per unit cross section measured in the units of $c\mu_1^2 T_1/(8\pi)$. Below, for brevity the quantity W_l is simply called energy.

According to the theory of self-induced transparency (SIT) on nondegenerate levels, a bell-shaped pulse decays in a medium if its 'area' satisfies the condition $\Theta_1 < \pi$ [24]. In the case of SIT on the degenerate $J = 0 \leftrightarrow J = 1$ transition [25], this condition is valid when the area of the input bell-shaped elliptically polarised pulse is defined by the expression

$$\Theta_1 = \int_{-\infty}^{+\infty} a_{10}(w)\sqrt{1 + \gamma_{10}^2}\,\mathrm{d}w. \tag{6}$$

For linearly and circularly polarised radiations, expression (6) in the case of the bell-shaped dependence $a_{10}(w)$ coincides with the pulse area in the theory of SIT on a nondegenerate quantum transition.

3. Results of calculations

3.1. Let us set in (5)

$$\alpha_{10} = 0.5,\ \gamma_{10} = 0,\ a_{10} = 0.8\,\mathrm{sech}(w - 7),$$

$$\alpha_{20} = -0.1,\ \gamma_{20} = -1,$$

$$a_{20} = 2.46\{\tanh[(w - 6)/2] + \tanh[(-w + 54)/2]\}.$$

Here, we have a linearly polarised bell-shaped input high-frequency radiation pulse, for which $\Theta_1 = 0.8\pi$. The input low-frequency radiation is a left-hand circularly polarised pulse with a flat top, which is smoothly switched on before the arrival of the high-frequency pulse and smoothly switched off after the end of the latter. Such an order in the application of input pulses is called the contraintuitive sequence in the EIT theory [6], high-frequency and low-frequency radiations being called probe and controlling radiations, respectively. The low-frequency pulse intensity in the region of its flat top is in this case 25 times higher than the maximum intensity of the high-frequency pulse.

The dependences $I_1(w)$ and $I_2(w)$ are presented in Fig. 1 for different distances s. Because changes of I_2 during the propagation of low-frequency radiation in a medium are comparatively small and are manifested only in the upper part of the curve, the dependences for I_2 are presented in the region $I_2 \geqslant 11$.

The calculation showed that the high-frequency pulse decomposes in the medium into two separate pulses [pulses (*1*) and (*2*) in Figs. 1b–d]. In this case, the high-frequency radiation energy weakly decreases during propagation, approximately 1.5 times at a distance of $s = 30$. Note that if high-frequency radiation were absent, then, as follows from calculations, the high-frequency pulse energy for $\Theta_1 = 0.8\pi$ at this distance would decrease almost by a factor of 800.

The evolution of the PE parameters for the high-frequency pulse at a distance of $s = 30$ is shown in Fig. 2. According to the dependence of a_1, the high-frequency pulse decomposes into pulses (*1*) and (*2*) corresponding to pulses (*1*) and (*2*) in Fig. 1d. Between these pulses, weak short closely spaces pulses are located, and pulse (*2*) is followed by another weak and long pulse. (These weak pulses are unnoticeable at the scale of Fig. 1d.)

In the region of pulse (*1*), we have $\gamma_1 = 1$. This means that after the decomposition of the input low-frequency pulse into component pulses, which occurs, as follows from Fig. 1, for $s > 7$, the first pulse has the right-hand circular polarisation. Recall that the input high-frequency pulse is linearly polarised. The value of γ_1 in the region of pulse (*2*) is close to –1, as in the region of the third pulse. Therefore, pulse (*2*) and the third pulse have in fact left-hand circular polarisations. During each weak pulse located between

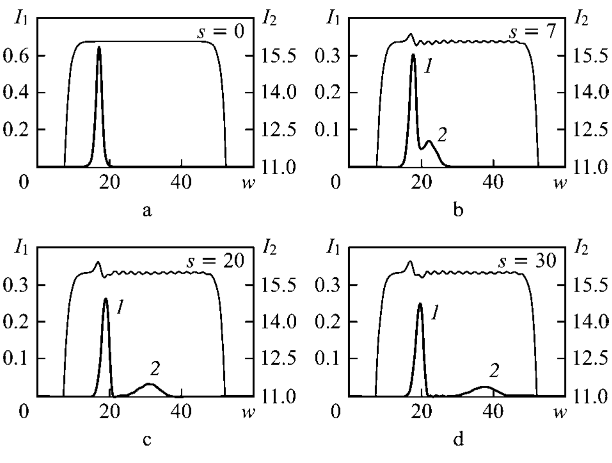

Figure 1. Evolution of the intensities I_1 (thin curves) and I_2 (thick curves) of high-frequency and low-frequency radiations, respectively, for different values of s.

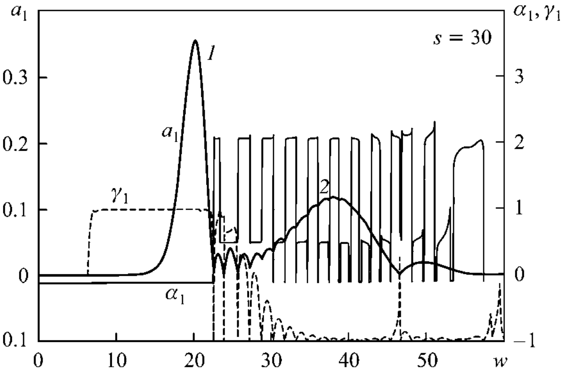

Figure 2. Evolution of PE parameters for the high-frequency pulse for $s = 30$.

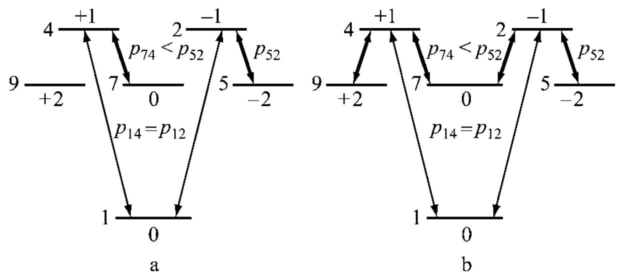

Figure 3. Schemes of quantum transitions. The numbers to the left of horizontal straight lines are the numbers of states, the numbers at the top or bottom indicate the quantum number M of the corresponding states; (a) calculations in section 3.1, (b) calculations in section 3.2.

pulses (*1*) and (*2*), polarisation changes from the left-hand circular ($\gamma_1 = -1$) to the left- or right-hand elliptical. The dependence for α_1 shows that this angle increases jump-wise by $\pi/2$ from 0.5 at the input plane and then, also jump-wise, returns to its value at the instants when the PE transforms to a circle ($\gamma_2 = -1$). Such a jump means the transformation of the major axis of the PE to the minor axis during the passage through the stage of circular polarisation.

We treat the pulsed structure obtained in this calculation as the complicated shape of an adiabaton in the case of elliptically polarised input radiations. Because the high-frequency pulse decomposes into two well separated pulses, this structure can be called a double adiabaton. The concept of the adiabaton was proposed in the study of the specific manifestation of EIT in the Λ-scheme for nondegenerate energy levels in the case of circular or collinear linearly polarised radiations. According to [6], the adiabaton is a pair of high-frequency and low-frequency pulses, appearing if the intensities of input high-frequency and low-frequency radiations have the form shown in Fig. 1a. The high-frequency component of the usual adiabaton propagates in a medium without the energy loss and without changing the bell-shaped envelope. On the plateau of the low-frequency component of the adiabaton, a hump is formed, which is followed by a dip located in the region of the high-frequency component [6]. The leading and trailing edges of the low-frequency component of the adiabaton and the hump on its plateau propagate at the speed of light in vacuum. The propagation velocities of the high-frequency component and the dip on the plateau of the low-frequency component are smaller, and, as the peak value of the high-frequency component, they decrease with decreasing the Rabi frequency of the low-frequency component of the adiabaton.

Returning to current calculations, note that linearly polarised high-frequency radiation ($\gamma_{10} = 0$) incident on the medium can be represented by a sum of components with left- and right-hand circular polarisation. Quantum transitions excited by these components are shown in Fig. 3a by the arrows tilted to the left and right, respectively. The thick arrows in Fig. 3a indicate quantum transitions excited by high-power low-frequency radiation with the left-hand circular polarisation ($\gamma_{20} = -1$).

It is reasonable to assume that the evolution of the left-hand circularly polarised component high-frequency radiation in the medium is determined by EIT in the Λ-scheme of levels 1, 7, 4, while the evolution of right-hand circularly polarised component – in the Λ-scheme of levels 1, 5, 2. In the first case, an adiabaton with the left-hand circularly polarised high-frequency and low-frequency components should appear, while in the second one – with the right-hand circularly polarised high-frequency component and left-hand circularly polarised low-frequency component.

The low-frequency radiation fields (controlling fields in the EIT theory) in these Λ-schemes are identical. The moduli p_{52} and p_{74} of the electric dipole moments of these transitions satisfy the relation $p_{52} = \sqrt{6}p_{74}$ [26]. Therefore, the Rabi frequency of the controlling field in the Λ-scheme of levels 1, 7, 4 is lower than that in the Λ-scheme of levels 1, 5, 2. Because of this, the left-hand circularly polarised high-frequency component of the adiabaton in the Λ-scheme of levels 1, 7, 4 has the smaller intensity and smaller propagation velocity than the right-hand circularly polarised high-frequency component of the adiabaton in the Λ-scheme of levels 1, 5, 2. Due to the difference in the velocities, the high-frequency components of adiabatons appearing in the two Λ-schemes are separated. This explains the two-pulse structure of high-frequency radiation obtained in calculations (Figs 1b–d).

Note that both pulses of the high-frequency component of the adiabaton presented in Figs 1 and 2 decay during their propagation deep in the resonance medium, whereas the high-frequency pulse of the classical adiabaton [6] propagates without the energy loss. This is explained by the fact that the adiabaton theory [6] is constructed assuming that the oscillator strengths of quantum transitions are identical and neglecting the inhomogeneous broadening of spectral lines.

3.2. In the case of linearly polarised input high-frequency and low-frequency pulses, the diagram of transitions has the form shown in Fig. 3b. The thick arrows correspond now to the right-hand and left-hand circularly polarised components of the input low-frequency radiation of the same intensity. It is obvious that in this case the left-hand and right-hand circularly polarised components of high-frequency radiation are under the same conditions, and a double adiabaton should not appear.

To elucidate how a double adiabaton transforms to a usual adiabaton described in [6] when the polarisation of the input low-frequency radiation changes from circular to linear, we performed additional calculations with the boundary conditions

$$\alpha_{10} = 0.5,\ \gamma_{10} = 0,\ a_{10} = 0.8\,\mathrm{sech}(w - 7),\ \alpha_{20} = 0.5,$$

$$\alpha_{20} = 2.46\sqrt{1 + \gamma_{20}^2}\{\tanh[(w - 6)/2] + \tanh[(-w + 54)/2]\}$$

for $\gamma_{20} = -0.5$, -0.25, and 0. The input high-frequency pulse and the intensity of the input low-frequency pulse in these calculations are the same as in section 3.1.

Figure 4a presents the dependences $W_1(s)$ of the low-frequency radiation energy for the values of γ_{20} indicated above and $\gamma_{20} = -1$. One can see that as $|\gamma_{20}|$ decreases, the losses of the high-frequency radiation energy decrease and become minimal when both radiations are linearly polarised.

Figure 4b presents the intensities of high-frequency radiation pulses at a large distance ($s = 30$) for $\gamma_{20} = -0.5$, -0.25, and 0 (the case $\gamma_{20} = -1$ is shown in Fig. 1d). As $|\gamma_{20}|$ decreases, the time interval between the pulses of the double adiabaton decreases, and when $\gamma_{20} = 0$, the high-frequency radiation is almost completely concentrated in one pulse accompanied by several weak pulses at its trailing edge. Our calculations showed that in this case the high-frequency radiation is linearly polarised ($\gamma_1 = 0$) in the same direction as the low-frequency pulse. Such a high-frequency pulse is similar to the high-frequency component of the usual adiabaton on nondegenerate quantum transitions [6].

The evolution of the PE parameters of the high-frequency radiation pulse at a distance of $s = 30$ for small $|\gamma_{20}|$ ($\gamma_{20} = -0.25$) is shown in Fig. 5. The leading front of the first pulse of the double adiabaton has the right-hand elliptic polarisation ($\gamma_{20} = 0.62$), while polarisation at the trailing edge of the pulse becomes left-hand elliptic, with variable γ_1. Recall that for $\gamma_{20} = -1$, the entire first pulse of the double adiabaton has the right-hand circular polarisation. In the region of the second pulse and low-intensity pulses, the trailing edge of the high-frequency pulse has mainly left-hand elliptic polarisation with variable parameter γ_1. At the instants when polarisation becomes circular, the major axis of the PE transforms to the minor axis (the angle α_2 changes jump-wise by $\pi/2$).

3.3. Note that if the values of γ_{20} are changed to opposite, the results of calculations presented in section 3 remain also valid when the sign of γ_2 is changed.

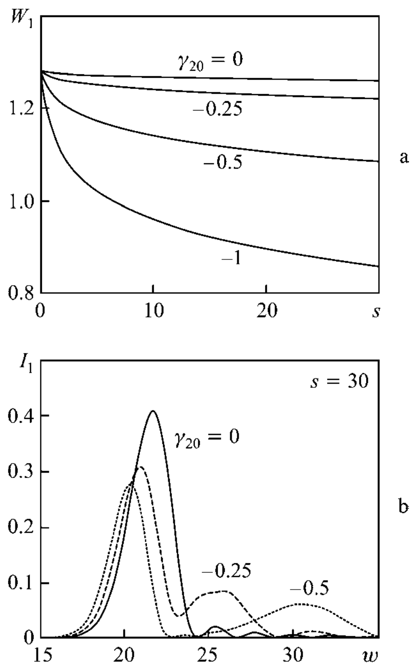

Figure 4. Dependences of the high-frequency radiation energy W_1 on s (a) and of the high-frequency radiation intensity I_1 on w for $s = 30$ (b).

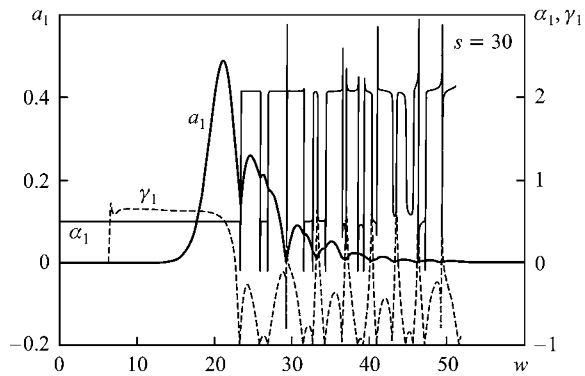

Figure 5. Evolution of the PE parameters for the high-frequency pulse for $s = 30$.

4. Dimensional estimates

Let us make estimates for the saturated vapour of the ^{208}Pb isotope at temperature 950 K. In this case $T_1 = 1.63 \times 10^{-10}$ s. By using the oscillator strengths for quantum transitions in the ^{208}Pb isotope [19] and the temperature dependence of the saturated vapour pressure for lead [27], we obtain $N = 3.4 \times 10^{13}$ cm^{-3} and $z_0 = 0.03$ cm. The quantities z_0 and T_1 are used as normalisation parameters on passing from the dimensional distance z and the dimensional time t to dimensionless variables s and w by expressions (3). Then, the duration of bell-shaped input pulses, specified in our calculations with the help of hyperbolic cosecant, will be approximately 0.4 ns. The exact value of the duration of the input low-frequency pulse with a flat top used in calculations is obviously insignificant. The duration of this pulse should only considerably exceed the duration of the input high-frequency pulse. Note that the value of z_0 strongly depends on the absolute temperature. Thus, $z_0 = 0.1$ cm at 900 K and 0.01 cm at 1000 K. The value of T_1, on the contrary, very weakly depends on the absolute temperature: $T_1 = 1.68 \times 10^{-10}$ s at 900 K and 1.59×10^{-10} at 1000 K.

The dimensional intensities of low-frequency and high-frequency radiations (in kW cm^{-2}, $\bar{I}_1$ and $\bar{I}_2$, respectively) can be estimated from the expression $\bar{I}_l = 1.3 I_l$, $l = 1, 2$. The calculation by this expression in section 3.1 gives the maximum intensity of the input high-frequency radiation equal to 0.84 kW cm^{-2} and the intensity of the flat top of the input low-frequency radiation pulse equal to 20.9 kW cm^{-2}.

By using oscillator strengths for the ^{208}Pb isotope [19], we can easily estimate the relaxation times of the quantum transitions under study. The shortest of these times is 10 ns. Because low-frequency radiation acts on a quantum transition with initially unpopulated levels, each atom experiences perturbation only when it is simultaneously excited by low-frequency and high-frequency pulses. The duration of this perturbation coincides with that of the low-frequency pulse. The latter, as noted above, is 0.4 ns, which means that the influence of irreversible relaxation can be neglected.

5. Conclusions

We have shown that if a high-power input low-frequency pulse with a flat top and a long enough duration is applied contraintuitively on a weak bell-shaped input high-frequency pulse of small duration, an adiabaton of a new type can appear. The high-frequency component of this adiabaton consists of two circular polarised pulses with electric-field strength vectors rotating in the opposite directions and with different propagation velocities.

These results, according to calculations, which are omitted here, remain valid for input high-frequency pulses of different shapes and durations under the condition that their spectral widths differ no more than 2 – 3 times from the spectral width of the resonance quantum transition with a higher frequency in the Λ-scheme under study. In this case, the duration of the input low-frequency pulse with a flat top should considerably exceed the duration of the input high-frequency radiation pulse. An increase (decrease) in the spectral width of the input high-frequency pulse leads to the increase (decrease) of distances at which the described effects can be observed.

The calculations preformed in the paper assumed that the frequency of each input pulse coincided with the central frequency of the corresponding quantum transition. The abandonment of this restriction may become the main direction of further investigations of the nonstationary double resonance of elliptically polarised pulses on degenerate quantum transitions.

References

1. Konopnicki M.J., Eberly J.H. *Phys. Rev. A*, **24**, 2567 (1981).
2. Stroud C.R., Cardimona D.A. *Opt. Commun.*, **37**, 221 (1981).
3. Acherhalt J.R., Milonni P.V. *Phys. Rev. A*, **33**, 3185 (1986).
4. Bol'shov L.I., Elkin N.N., Likhanskii V.V., Persiantsev M.I. *Pis'ma Zh. Eksp. Teor. Fiz.*, **39**, 360 (1984).
5. Harris S.E. *Phys. Rev. Lett.*, **70**, 552 (1993).
6. Grobe R., Eberly J.H. *Laser Phys.*, **5**, 542 (1995).
7. Fitzgerald R. *Phys. Today*, **52**, 17 (1999).
8. Fleischhauer M., Lukin M.D. *Phys. Rev. A*, **65**, 022314 (2002).
9. Arkhipkin V.G., Timofeev I.V. *Pis'ma Zh. Eksp. Teor. Fiz.*, **76**, 74 (2002).
10. Tarak N.D., Agarwal G.S. *Phys. Rev. A*, **67**, 033813 (2003).
11. Lukin V.D. *Rev. Mod. Phys.*, **75**, 457 (2003).
12. Eberly J.H., Rahman A., Grobe R. *Laser Phys.*, **6**, 69 (1996).
13. Eisaman M.D., Childress L., Andre A., Massou F., Zibrov A.S., Lukin M.D. *Phys. Rev. Lett.*, **93**, 233602 (2004).
14. Arkhipkin V.G., Timofeev I.V. *Dokl. Ross. Akad. Nauk*, **401**, 467 (2005).
15. Basharov A.M., Maimistov A.I. *Zh. Eksp. Teor. Fiz.*, **94**, 61 (1988).
16. Basharov A.M., Maimistov A.I. *Opt. Spektrosk.*, **68**, 1112 (1990).
17. Kasapi A., Maneesh J., et al. *Phys. Rev. Lett.*, **74**, 2447 (1995).
18. Volkov A.V., Druzhinina M.A., Parshkov O.M. *Kvantovaya Elektron.*, **39**, 845 (2009) [*Quantum Electron.*, **39**, 845 (2009)].
19. De Zafra R.L., Marshall A. *Phys. Rev.*, **170**, 28 (1968).
20. Fleischhauer M., Imamoglu A., Marangos J.P. *Rev. Mod. Phys.*, **77**, 633 (2005).
21. Akhmanov S.A., Khokhlov R.V. *Problemy nelineinoi optiki, 1961 – 1963* (Problems of Nonlnear Optics, 1961 – 1963) (Moscow: Izd. Akad. Nauk SSSR, 1965).
22. Butylkin V.S., Kaplan A.E., Khronopulo Yu.G., Yakubovich E.I. *Rezonansnye vzaimodeistviya sveta s veshchestvom* (Resonance Interactions of Light with Matter) (Moscow: Nauka, 1977).
23. Born M., Wolf E. *Principles of Optics* (Oxford: Pergamon Press, 1969; Moscow: Nauka, 1970).
24. McCall S.L., Hahn E.L. *Phys. Rev.*, **183**, 457 (1968).
25. Basharov A.M., Maimistov A.I. *Zh. Eksp. Teor. Fiz.*, **87**, 1594 (1984).
26. Sobel'man I.I. *Vvedenie v teoriyu atomnykh spektrov* (Introduction to the Theory of Atomic Spectra) (Moscow: Nauka, 1977).
27. Grigor'ev I.S., Meilikhov E.Z. (Eds) *Fizicheskie velichiny. Spravochnik* (Handbook of Physical Quantities) (Moscow: Energoatomizdat, 1991).